

AFD-Net: Adaptive Fully-Dual Network for Few-Shot Object Detection

Longyao Liu, Bo Ma, Yulin Zhang, Xin Yi, Haozhi Li
Beijing Institute of Technology

roell.liu@bit.edu.cn

Abstract

Few-shot object detection (FSOD) aims at learning a detector that can fast adapt to previously unseen objects with scarce annotated examples, which is challenging and demanding. Existing methods solve this problem by performing subtasks of classification and localization utilizing a shared component (e.g., RoI head) in a detector, yet few of them take the preference difference in embedding space of two subtasks into consideration. In this paper, we carefully analyze the characteristics of FSOD and present that a general few-shot detector should consider the explicit decomposition of two subtasks, and leverage information from both of them for enhancing feature representations. To the end, we propose a simple yet effective Adaptive Fully-Dual Network (AFD-Net). Specifically, we extend Faster R-CNN by introducing Dual Query Encoder and Dual Attention Generator for separate feature extraction, and Dual Aggregator for separate model reweighting. Spontaneously, separate decision making is achieved with the R-CNN detector. Besides, for the acquisition of enhanced feature representations, we further introduce Adaptive Fusion Mechanism to adaptively perform feature fusion suitable for the specific subtask. Extensive experiments on PASCAL VOC and MS COCO in various settings show that, our method achieves new state-of-the-art performance by a large margin, demonstrating its effectiveness and generalization ability.

1. Introduction

Recent years have witnessed impressive advances of CNNs [17, 9, 18] in object detection [32, 30, 8, 14, 23, 29, 4, 13]. However, training general object detection models from scratch typically requires rich labeled data which is extremely expensive to obtain or even hard to collect, such as endangered animals. Thus, detectors significantly suffer a performance drop when training examples are inadequate [45]. On the contrary, humans exhibit a strong ability to address this issue: even a child can easily learn to recognize novel characteristics from only a few instances [34].

This triggers recent researches on few-shot learning

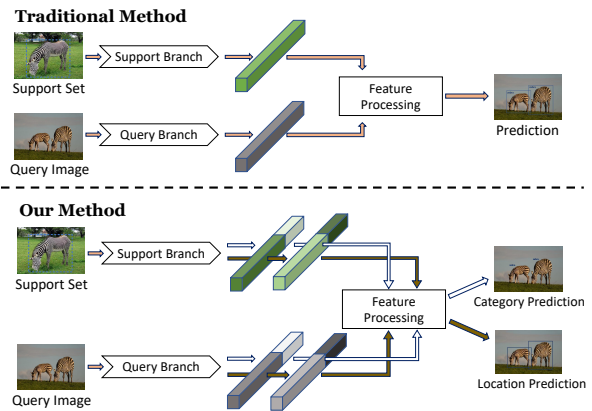


Figure 1. Comparison of our framework and traditional methods. Our Adaptive Fully-Dual Network decomposes the processing of classification and localization in FSOD, with novel feature fusion mechanism for effectively encoding query image and support set.

(FSL). It is considered promising to enhance the generalization ability of deep networks from limited training examples [22, 37, 11, 25, 1]. Concretely, FSL aims at recognizing instances from novel classes given only a few annotated data per category in the inference stage, with the availability of abundant labeled training samples from base classes. However, most researches in few-shot learning community focus on image classification [21, 37, 35, 36, 12, 27], while far less progress has been made in the field of object detection [19, 44, 42], which is generally considered much more challenging due to the existence of an additional subtask, specifically, few-shot localization, besides the subtask of object recognition.

A trend to solve FSOD is to conjoin a reweighting module with a base object detector, e.g., Faster R-CNN [32]. Concretely, these few-shot detectors [44, 42] introduce an additional branch to extract discriminative features of support set from novel classes, and then use these class-attentive vectors to reweight RoI (Region-of-Interest) head **shared** for subsequent estimation of object categories and locations. However, classification and localization are two subtasks in FSOD. The former subtask focuses on providing a coarse location of the object via classification, while the

latter aims at estimating an accurate object state by a refined bounding box [43]. This leads to their distinct preferences towards feature representations. In other words, generated features suitable for classification are probably not suitable for bounding box regression. Meanwhile, these two subtasks are complementary [41], thus leveraging the information from unfocused tasks is crucial to enhance the representation ability of few-shot detectors.

Motivated by the abovementioned analysis, we present that a general few-shot detector should: 1) decompose the processing of classification and localization in FSOD with specific processing for the specific subtask, involving feature representations, model reweighting and decision making; 2) consider efficient feature fusion between two subtasks for effectively encoding both query image and support set, as shown in Fig. 1.

In this paper, we propose a novel framework for FSOD, namely *Adaptive Fully-Dual Network (AFD-Net)*, as illustrated in Fig.2. Specifically, we extend Faster R-CNN by introducing three modules, *i.e.*, Dual Query Encoder (DQE), Dual Attention Generator (DAG), and Dual Aggregator (DA) for separate processing of two subtasks, together with Adaptive Fusion Mechanism (AFM) for the acquisition of enhanced feature representations. DQE and DAG are designed for separate feature representations in two subtasks. Query features are encoded by DQE into two groups of RoI vectors, where each group is obtained following the guidance of AFM and is used for a particular subtask. In parallel with DQE, DAG encodes support features into class-attentive vectors with the same scheme in feature representation. DA performs separate model reweighting using two aggregators, where each RoI vector from query features is aggregated with each class-attentive vector from support features in each aggregator assigned the specific subtask. Finally, a R-CNN detector is applied to estimate the object location and category respectively, realizing separate decision making, spontaneously.

Extensive experiments on two public datasets in various settings show that despite its simplicity, our method outperforms existing state-of-the-art approaches by a large margin, which demonstrates its effectiveness. To summarize, the main contributions of this paper are three-fold:

- We propose a simple yet effective framework for few-shot object detection. To the best of our knowledge, we are among the first to solve FSOD by decomposing the processing of classification and localization.
- We further introduce three modules, *i.e.*, DQE, DAG and DA, to perform decomposition in multiple components of our network, along with AFM for enhanced feature representations.
- Our proposed method achieves a new state-of-the-art performance on multiple benchmarks.

2. Related Work

General Object Detection. Recent object detectors based on deep CNNs can be mainly divided into two steams, *i.e.*, one-stage detectors and two-stage ones. R-CNN series [14, 13, 32, 16, 8, 23] belong to the first category, which generate region proposals [32] of potential objects in the first stage, and then perform category and bounding box estimation at the proposal-level. On the contrary, YOLO [29] and the variants [30, 24, 31, 3] dominate the one-stage steam. These methods use a single CNN to predict categories and locations of the objects directly, without explicitly generating proposals. These two branches of general object detectors unanimously depend on a huge amount of data with elaborate bounding box annotations. When training samples are limited, they struggle heavily.

Few-shot Learning. Few-shot learning refers to learning to learn general knowledge that can be easily transferred to new tasks with only a handful of annotated examples [22, 37, 1]. Few-shot classification has recently been widely investigated as a representative task of few-shot learning. Generally, solutions to this problem involve two groups: meta-learning based and fine-tuning based methods. The former can be further categorized into: 1) metric-learning based methods [21, 35, 36] that focus on the similarity of input images on the embedding space; 2) optimization-based ones [28, 11, 25], where a meta-learner is designed to simulate the optimization process for the fast adaptation to novel classes with limited samples; 3) model-based methods [2, 12, 39] that aim to estimate the network parameters for novel tasks with the help of a learned predictor. Fine-tuning based approaches [6, 7] demonstrate that simple fine-tuning techniques are crucial and effective towards few-shot learning. While substantial progress has been made in few-shot classification, the problem of few-shot object detection is relatively unsolved due to its complexity for the existence of additional localization task.

Few-shot Object Detection. There are several attempts to solve the problem of few-shot object detection. LSTD [5] applies transfer learning technique in object detection with limited examples and demonstrates its effectiveness. TFA [38] proposes that only fine-tuning the last layer of existing detectors is crucial and effective despite its simplicity. Metric learning widely explored in few-shot classification can be extended to few-shot object detection. For example, RepMet [20] scores the pair-wise similarity between embedded features of input query and support images. [10] incorporates attention mechanism into RPN (Region Proposal Network) and explicitly defines a multi-relation detector to suppress detection of the background. Recently, methods based on meta-learning have been a popular trend. FSRW [19] attaches a reweighting module with YOLOv2 [30] to adjust the full input image features using class-attentive vectors of support images,

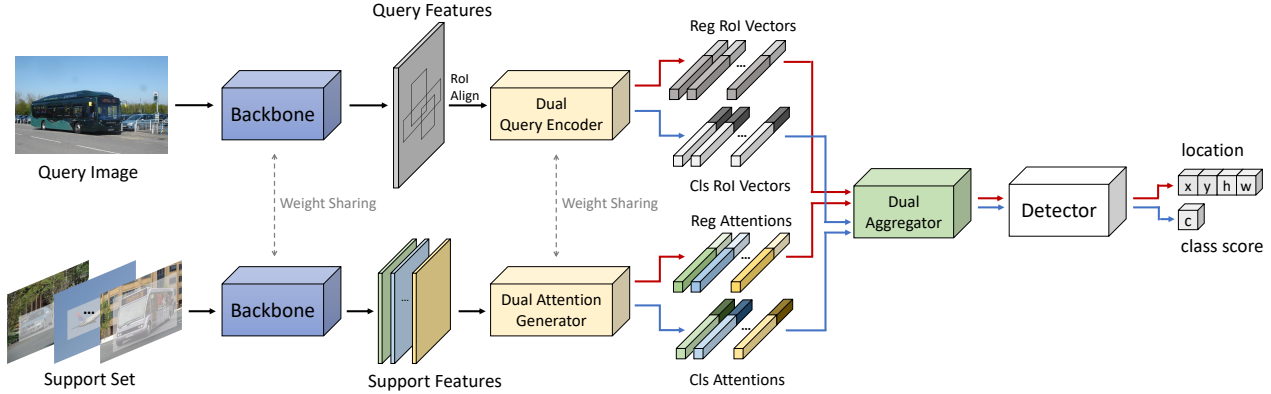


Figure 2. The architecture of Adaptive Fully-Dual Network for few-shot object detection. It consists of three key components: 1) the query branch receives a query image and generates its RoI vectors; 2) the support branch encodes support set into its class-attentive vectors; 3) two groups of features from two branches are aggregated for performing category and location estimation with a R-CNN detector. We further introduce three modules, *i.e.*, Dual Query Encoder, Dual Attention Generator and Dual Aggregator in three components, along with Adaptive Fusion Mechanism for enhanced feature representations. Note that all these three modules are in a dual architecture, where each path performs a specific subtask. Black line represents shared path for two subtasks, red and blue lines represent bounding box regression and classification subtasks, respectively.

while Meta R-CNN [44] applies reweighting on RoI features based on Faster R-CNN [32]. MetaDet [40] presents a meta-model to predict the parameters of category-agnostic and category-specific components in a detector, separately. FSDetView [42] applies a slightly more complicated feature aggregation scheme to further improve the detection performance and evaluation reliability.

3. Methodology

In this section, we first introduce the setup for few-shot object detection in Section 3.1. Then we elaborate on our proposed approach in Section 3.2. Finally, the detailed training procedure is provided in Section 3.3.

3.1. Problem Setup

As in previous work [19, 44, 42], we adopt the following few-shot object detection settings. In the training phase, we are provided with two training sets, *i.e.*, a base set D_{base} from base classes C_{base} with abundant instances and a novel set D_{novel} from novel classes C_{novel} with only a few samples per category, where C_{base} and C_{novel} are non-overlapping, *i.e.*, $C_{base} \cap C_{novel} = \emptyset$. For each sample $(x, y) \in D_{base} \cup D_{novel}$, $x = \{obj_i\}_{i=1}^N$ is an image containing N objects, and $y = \{(cls_i, box_i)\}_{i=1}^N$ denotes N categories $\{cls_i\}_{i=1}^N$ with each $cls_i \in C_{base} \cup C_{novel}$ and N structured annotations $\{box_i\}_{i=1}^N$ of the N objects in the image x . The aim of the few-shot object detector is to classify and locate objects from both novel and base classes in an image with only K (usually less than 10) available instances per class in the phase of inference, with the help of transferable knowledge learned from abundant examples from base classes.

3.2. Adaptive Fully-Dual Network

Our proposed framework decomposes the processing of few-shot classification and localization, as well as enhances feature representations. We adopt the widely used two-stage detector Faster R-CNN [32] as the base model, which first generates RoIs of potential objects, and then performs detection using a single RoI head. The overall architecture of our proposed network is demonstrated in Fig. 2. Concretely, we extend Faster R-CNN to a dual Siamese architecture suitable for the few-shot object detection scenario, where a query image is encoded by the upper Faster R-CNN branch, and the other branch for support set. Each branch further contains two paths, where each path performs feature extraction for the specific subtask. Query RoI vectors and class-attentive vectors of support set from two branches are then aggregated, achieving the reweighting of Faster R-CNN for the subsequent detection of novel instances. We introduce Dual Query Encoder (DQE) and Dual Attention Generator (DAG) for separate feature representations, and Dual Aggregator (DA) for separate model reweighting based on our proposed architecture. Furthermore, we present Adaptive Fusion Mechanism (AFM) to effectively encode both the query image and support set.

3.2.1 Dual Query Encoder

In two-stage object detectors, RPN is applied to generate class-agnostic RoIs. These RoIs are then utilized to perform object detection by a R-CNN detector. Instead of generating a single group of RoI vectors $\{r_i\}_{i=1}^n$ of the input query image q by a single RoI head in previous work [44, 42],

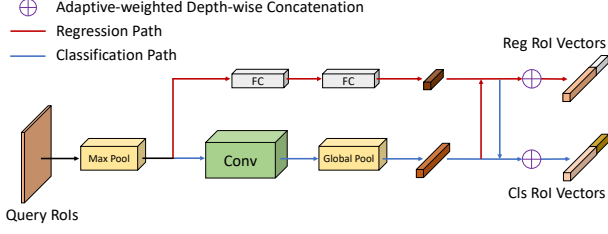


Figure 3. Illustration of Dual Query Encoder.

we propose Dual Query Encoder (DQE) that generates two groups of RoI vectors $\{r_i^t\}_{i=1}^n$ with $t \in \{cls, reg\}$ of the input query image for subtasks of classification and bounding box regression respectively, guided by our observation that subtasks of classifying and locating objects in few-shot detection should be treated separately. In particular, DQE involves two parallel branches, where each branch encodes input query RoIs into RoI vectors for the specific task t , as shown in Fig. 3. This procedure is formulated as below:

$$\{r_i^t\}_{i=1}^n = E^t(\psi(\varphi(q))), t \in \{cls, reg\} \quad (1)$$

where q denotes input query image in Fig. 2, $\varphi(\cdot)$ denotes the backbone network of Faster R-CNN, $\psi(\cdot)$ denotes the RoIAlign operation, $E^t(\cdot)$ denotes feature extraction of the specific branch in DQE, t denotes the specific subtask, *i.e.*, *cls* for classification and *reg* for bounding box regression, and n denotes the number of RoI vectors in each group.

We adopt a two-layer fully-connected (*2-fc*) encoder in regression branch and a convolution (*conv*) encoder in classification branch. Furthermore, we consider using the information from the unfocused branch to enhance the feature representations in each branch. Output task-specific RoI vectors from each branch are the weighted concatenation of *fc* features and *conv* features, where the weights can be adaptively adjusted according to the specific task and their values indicate the contributions of each group of RoI vectors to the integrated task-specific RoI vectors, which is the key philosophy of **Adaptive Fusion Mechanism (AFM)**. Thus $E^t(\cdot)$ in Eq. (1) can be rewritten as:

$$E^t(\cdot) = [\lambda_{conv}^t E_{conv}^t(\cdot), \lambda_{fc}^t E_{fc}^t(\cdot)], t \in \{cls, reg\} \quad (2)$$

where $E_{conv}^t(\cdot)$ and $E_{fc}^t(\cdot)$ denote *conv* encoder and *fc* encoder respectively for the specific subtask $t \in \{cls, reg\}$, λ_{conv}^t and λ_{fc}^t denote the learnable weights of corresponding task-specific RoI vectors and are initialized to 1, $[\cdot, \cdot]$ denotes the depth-wise concatenation operation.

3.2.2 Dual Attention Generator

A popular scheme to solve FSOD is first encoding support set into class-attentive vectors, and then using them to reweight the base detector [19, 44, 42]. These vectors from support set can be regarded as the attentions of corresponding objects in the query image. The encoding process is performed by the support branch in Fig. 2. We

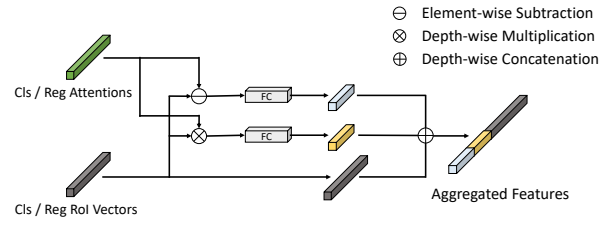


Figure 4. Illustration of feature aggregation scheme.

further exploit this scheme, leading to our proposed Dual Attention Generator (DAG). DAG is designed in the same structure with DQE for the effectiveness of model reweighting, thus we omit its illustration for simplicity. It receives support set $\{s_j\}_{j=1}^m$ from m categories as input and generates two groups of class-attentive vectors $\{a_j^t\}_{j=1}^m$ with $t \in \{cls, reg\}$ for two subtasks respectively:

$$\{a_j^t\}_{j=1}^m = G^t(\varphi(\{s_j\}_{j=1}^m)), t \in \{cls, reg\} \quad (3)$$

where $\varphi(\cdot)$ denotes the backbone network in support branch sharing parameters with query branch in Fig. 2, $G^t(\cdot)$ denotes the attention generation operation of the task-specific path in DAG for subtask t .

Similar to Dual Query Encoder, $G^t(\cdot)$ in Eq. (3) can be rewritten as:

$$G^t(\cdot) = [\lambda_{conv}^t G_{conv}^t(\cdot), \lambda_{fc}^t G_{fc}^t(\cdot)], t \in \{cls, reg\} \quad (4)$$

where $G_{conv}^t(\cdot)$ and $G_{fc}^t(\cdot)$ denote *conv* and *fc* attention generators respectively for the specific subtask t , λ_{conv}^t and λ_{fc}^t are shared with those in DQE, and the depth-wise concatenation $[\cdot, \cdot]$ here is also an adaptive-weighted operation.

3.2.3 Dual Aggregator

In this paper, besides separate feature representations for two subtasks, we decompose the processing of feature aggregation to realize separate model reweightings, leading to our Dual Aggregator (DA). DA consists of a classification aggregator and a bounding box regression aggregator in parallel. In each aggregator, each RoI vector of query features is aggregated with each class-attentive vector of support features following the scheme introduced in [42], as shown in Fig. 4, which can be formulated as:

$$\begin{aligned} \{f_k^t\}_{k=1}^{n \times m} &= A^t(\{r_i^t\}_{i=1}^n, \{a_j^t\}_{j=1}^m) \\ &= \left\{ [r_i^t \otimes a_j^t, r_i^t - a_j^t, r_i^t]_k^t \right\}_{k=1}^{n \times m}, t \in \{cls, reg\} \\ &\text{for each } i \in \{1, 2, \dots, n\}, j \in \{1, 2, \dots, m\} \end{aligned} \quad (5)$$

where $\{f_k^t\}_{k=1}^{n \times m}$ denotes aggregated features from the aggregator assigned the specific subtask t , $A^t(\cdot, \cdot)$ denotes the aggregation of RoI vectors and class-attentive vectors for subtask t , \otimes denotes the depth-wise multiplication.

The separate two groups of aggregated features $\{f_k^t\}_{k=1}^{n \times m}$ with $t \in \{cls, reg\}$ are then provided to the classifier and regressor in R-CNN detector respectively, to obtain the estimated category and location. As the input features of the detector are divided into two groups distinct from prior methods, the decision making in our framework is decomposed as well.

3.3. Training Procedure

3.3.1 Training Phase

Following the common practice in [19, 44, 38, 42], we train our network in two phases. Base data D_{base} from base classes C_{base} with abundant samples per class are used to train the model in the first base training phase. Then the balanced base data D_{base} and novel data D_{novel} with only K samples per class are fed into the network in the second fine-tuning phase for the fast adaptation to novel classes.

3.3.2 Training Data Organization

In the training phase, distinct from general object detectors that applying an image x_i as the training mini-batch, our few-shot detector applies a task T_i as an input training data in the meta-learning paradigm [19, 44, 42]. Each input task $T_i = S_i \cup Q_i$ is the union of a query set Q_i and a support set S_i , where Q_i is provided to query branch in Fig. 2 is a query image q_i containing objects from m classes $C_i^{meta} \subseteq C_{base} \cup C_{novel}$, and S_i for support branch contains m K -shot ($K = 200$ in the base training phase and $K = \{1, 2, 3, 5, 10\}$ in the fine-tuning phase) clusters $\{g_i^p\}_{p=1}^m$, where each cluster g_i^p includes K images $\{s_{i,j}^p\}_{j=1}^K$ in the category p . Each support image $s_{i,j}^p$ is depth-wise concatenated with a structured binary $mask_{i,j}^p$ (see the input support set in Fig. 2, only one object is considered when multiple objects are present within an image).

3.3.3 Loss Function

We optimize our network in both training phases using the same loss function introduced in [44]:

$$L = L_{Faster\ R-CNN} + L_{meta} \quad (6)$$

where $L_{Faster\ R-CNN}$ denotes the loss function of base detector Faster R-CNN, involving the RPN loss, and classification loss together with bounding box regression loss for the decision making, L_{meta} denotes a meta loss aiming at encouraging attention features of support set to distinguish with each other.

Since our proposed DAG and DQE are in a dual architecture, L_{meta} in this paper is a sum of two components for classification and regression respectively. Thus the loss function in Eq. (6) can be precisely written as:

$$L = L_{Faster\ R-CNN} + L_{meta-cls} + L_{meta-reg} \quad (7)$$

where $L_{meta-cls}$ and $L_{meta-reg}$ denote the meta losses for classification and regression subtasks, respectively.

4. Experiments

In this section, we evaluate the effectiveness of our proposed few-shot object detector. We first introduce the experimental settings in Section 4.1. Then we present comparison results with recent SOTAs on multiple benchmarks in Section 4.2, and analyze the performance of information fusion in Section 4.3. Finally, we provide relative ablations to obtain a comprehensive understanding of our method in Section 4.4.

4.1. Experimental Settings

Benchmarks. We evaluate our method on general object detection benchmarks, *i.e.*, PASCAL VOC 2007, 2012 and MS COCO, in few-shot detection settings. As for PASCAL VOC, we follow the common practice in previous work [19, 44, 38, 42] and use train/val sets of VOC 07 and 12 for training while the test set of VOC 07 for testing. This benchmark covers 20 object categories, where 15 of them are regarded as base classes for the base training phase and the remaining 5 categories with only K ($K = \{1, 2, 3, 5, 10\}$) samples per class are considered as novel classes for few-shot fine-tuning phase. For the fair quantitative comparison, we adopt the same three class splits provided in [19]. For the evaluation protocol, we use mean Average Precision (mAP) of novel objects and the Intersection of Union (IoU) is set as 0.5 (AP_{50}). Another benchmark we evaluate on is MS COCO, which has 80k train images and 40k validation images, covering 80 classes. Among them, we denote the 20 classes overlapped with PASCAL VOC as novel classes with K ($K = \{10, 30\}$) samples per category and the rest 60 classes as base classes. We use 5k images from validation set for evaluation with the standard COCO-style evaluation metrics [24, 31] and the rest for training. To compare empirically, on both datasets, we evaluate on novel classes over 10 repeated runs and report the average performance.

Baselines. In our experiments, we compare our approach with two groups of baselines: meta-learning based methods, *i.e.*, FSRW [19], MetaDet [40], Meta R-CNN [44], FSOD [10], and FSDetView [42] along with transfer learning based methods, which can be further divided into: 1) attempts focusing on domain transfer, *e.g.*, LSTD [5]; 2) jointly training base detectors with base and novel objects without fine-tuning, denoted as YOLO/FRCN-joint [19, 44]; 3) first training base detectors with base objects and fine-tuning the entire model using novel objects with conditional iterations, denoted as YOLO/FRCN-ft [19, 44]; 4) training detectors in the same way as YOLO/FRCN-ft in the first phase yet fine-tuning the entire model until convergence, denoted as YOLO/FRCN-

Method / Shots	Novel Set 1					Novel Set 2					Novel Set 3				
	1	2	3	5	10	1	2	3	5	10	1	2	3	5	10
YOLO-joint [19]	0.0	0.0	1.8	1.8	1.8	0.0	0.1	0.0	1.8	0.0	1.8	1.8	1.8	3.6	3.9
YOLO-ft [19]	3.2	6.5	6.4	7.5	12.3	8.2	3.8	3.5	3.5	7.8	8.1	7.4	7.6	9.5	10.5
YOLO-ft-full [19]	6.6	10.7	12.5	24.8	38.6	12.5	4.2	11.6	16.1	33.9	13.0	15.9	15.0	32.2	38.4
FRCN-joint [44]	2.7	3.1	4.3	11.8	29.0	1.9	2.6	8.1	9.9	12.6	5.2	7.5	6.4	6.4	6.4
FRCN-ft [44]	11.9	16.4	29.0	36.9	36.9	5.9	8.5	23.4	29.1	28.8	5.0	9.6	18.1	30.8	43.4
FRCN-ft-full [44]	13.8	19.6	32.8	41.5	45.6	7.9	15.3	26.2	31.6	39.1	9.8	11.3	19.1	35.0	45.1
LSTD [5]	8.2	1.0	12.4	29.1	38.5	11.4	3.8	5.0	15.7	31.0	12.6	8.5	15.0	27.3	36.3
FSRW [19]	14.8	15.5	26.7	33.9	47.2	15.7	15.2	22.7	30.1	40.5	21.3	25.6	28.4	42.8	45.9
MetaDet [40]	18.9	20.6	30.2	36.8	49.6	21.8	23.1	27.8	31.7	43.0	20.6	23.9	29.4	43.9	44.1
Meta R-CNN [44]	19.9	25.5	35.0	45.7	51.5	10.4	19.4	29.6	34.8	45.4	14.3	18.2	27.5	41.2	48.1
TFA w/ fc [38]	22.9	34.5	40.4	46.7	52.0	16.9	26.4	30.5	34.6	39.7	15.7	27.2	34.7	40.8	44.6
TFA w/ cos [38]	25.3	36.4	42.1	47.9	52.8	18.3	27.5	30.9	34.1	39.5	17.9	27.2	34.3	40.8	45.6
FSDetView [42]	24.2	35.3	42.2	49.1	57.4	21.6	24.6	31.9	37.0	45.7	21.2	30.0	37.2	43.8	49.6
Ours	33.1	39.6	51.6	55.3	60.7	24.7	29.2	40.4	44.6	48.4	27.1	35.0	43.1	48.4	53.6

Table 1. Few-shot detection performance (AP_{50}) for novel categories on PASCAL VOC dataset. We evaluate baselines on three different novel sets. Our approach consistently outperforms other baselines by a large margin. **RED/BLUE** indicate SOTA/the second best. Reported results are averaged over multiple repeated runs.

ft-full [19, 44]; 5) training base detectors with base objects and fine-tuning only the last layer using novel objects, denoted as TFA w/fc [38] and TFA w/cos [38].

Implementation Details. Our proposed approach is implemented in the *PyTorch* [26] library. It employs the backbone network of ResNet [17] pre-trained on ImageNet [33] along with a RoIAlign [15] layer. Specifically, we use ResNet-101 on PASCAL VOC benchmark and ResNet-50 on MS COCO. Our model is trained end-to-end using a batch size of 4 on a single Nvidia GeForce GTX 1080Ti with 12 GB memory. For optimization, we keep the setups in [44, 42] on both benchmarks. Concretely, we adopt the SGD optimizer with an initial learning rate of 0.001, weight decay of 0.0005 and momentum of 0.9. The model is trained for 20 epochs in the base training phase and 9 epochs in the K -shot fine-tuning phase. The learning rate is reduced by 0.1 every 5 epochs in two training phases.

4.2. Comparison Results

PASCAL VOC. Our evaluation results are presented in Table 1. The comparison experiments cover few-shot object detection scenarios in five setups ($K = \{1, 2, 3, 5, 10\}$) across three base/novel set splits. As can be observed, our method outperforms recent state-of-the-art baselines by a large margin and obtains the best performance in all 15 cases. We notice that in the majority of cases, the improvements are much larger than the gap among previous approaches, which indicates the strong generalization ability of our model. Surprisingly, although the existence of high variance of support data in the extreme few-shot setup ($K = 1$), we obtain large improvements (+7.8% in the

Shots	Method	Base AP_{50}	Novel AP_{50}
3	LSTD [5]	66.3	12.4
	FSRW [19]	64.8	26.7
	Meta R-CNN [44]	64.8	35.0
	TFA w/ cos [38]	77.3	42.1
	FSDetView [42]	-	42.2
	Ours	67.9	51.6
10	LSTD [5]	66.3	38.5
	FSRW [19]	63.6	47.2
	Meta R-CNN [44]	67.9	51.5
	TFA w/ cos [38]	77.5	52.8
	FSDetView [42]	-	57.4
	Ours	70.6	60.7

Table 2. Few-shot detection performance (AP_{50}) for base and novel categories on Novel Set 1 of PASCAL VOC dataset. Our approach outperforms other baselines on novel classes and has a strong generalization ability. **RED/BLUE** indicate SOTA/the second best.

first split and +5.8% in the third split), showing the robustness of our method in tough scenarios. Besides, in the robust 10-shot setup, the improvements (+3.3% in the first split, +2.7% in the second split and +4% in the third split) are lower than those in other setups. This can be explained by that, as the number of instances per novel class increases, the sample variance decreases and the detection performance stabilizes.

Taking evaluation performance on base classes into consideration, we provide detailed results on the first base/novel split in Table 2. We can find that on base classes, recent fine-tuning based approach TFA [38] leads the per-

Shots	Method	Average Precision						Average Recall					
		0.5:0.95	0.5	0.75	S	M	L	1	10	100	S	M	L
10	LSTD [5]	3.2	8.1	2.1	0.9	2.0	6.5	7.8	10.4	10.4	1.1	5.6	19.6
	FSRW [19]	5.6	12.3	4.6	0.9	3.5	10.5	10.1	14.3	14.4	1.5	8.4	28.2
	MetaDet [40]	7.1	14.6	6.1	1.0	4.1	12.2	11.9	15.1	15.5	1.7	9.7	30.1
	Meta R-CNN [44]	8.7	19.1	6.6	2.3	7.7	14.0	12.6	17.8	17.9	7.8	15.6	27.2
	TFA w/ fc [38]	9.1	17.3	8.5	-	-	-	-	-	-	-	-	-
	TFA w/ cos [38]	9.1	17.1	8.8	-	-	-	-	-	-	-	-	-
	FSOD [10]	11.1	20.4	10.6	-	-	-	-	-	-	-	-	-
	FSDetView [42]	12.5	27.3	9.8	2.5	13.8	19.9	20.0	25.5	25.7	7.5	27.6	38.9
	Ours	16.9	32.8	15.8	4.9	18.5	27.1	23.9	30.8	31.1	11.7	33.1	45.8
30	LSTD [5]	6.7	15.8	5.1	0.4	2.9	12.3	10.9	14.3	14.3	0.9	7.1	27.0
	FSRW [19]	9.1	19.0	7.6	0.8	4.9	16.8	13.2	17.7	17.8	1.5	10.4	33.5
	MetaDet [40]	11.3	21.7	8.1	1.1	6.2	17.3	14.5	18.9	19.2	1.8	11.1	34.4
	Meta R-CNN [44]	12.4	25.3	10.8	2.8	11.6	19.0	15.0	21.4	21.7	8.6	20.0	32.1
	TFA w/fc [38]	12.0	22.2	11.8	-	-	-	-	-	-	-	-	-
	TFA w/cos [38]	12.1	22.0	12.0	-	-	-	-	-	-	-	-	-
	FSOD [10]	-	-	-	-	-	-	-	-	-	-	-	-
	FSDetView [42]	14.7	30.6	12.2	3.2	15.2	23.8	22.0	28.2	28.4	8.3	30.3	42.1
	Ours	18.6	35.0	17.9	5.6	19.8	29.2	25.5	33.0	33.3	14.1	35.5	47.3

Table 3. Few-shot detection performance for novel categories on MS COCO dataset. Our approach achieves an significant improvement over other baselines. **RED/BLUE** indicate SOTA/the second best. Reported results are averaged over multiple repeated runs.

formance, and our method obtains the best performance among other baselines. This is caused by that TFA is more like a general object detector focusing on detecting objects from base classes in the base training phase. Thus it suffers a more severe generalization problem (-35.2% in 3-shot setup and -24.7% in 10-shot setup) when adapted to novel classes. Compared with TFA, our method obtains a slighter performance drop (-16.3% in 3-shot setup and -9.9% in 10-shot setup), further demonstrating the generalization ability of our model.

MS COCO. We show the evaluation of 20 novel classes on MS COCO in 10/30-shot setups and report the standard COCO-style metrics in Table 3. Obviously, our approach significantly outperforms recent SOTAs in all setups, despite the complexity and a huge amount of data in MS COCO, verifying its effectiveness and robustness. Note that our method performs much better in detection of small objects in comparison with other SOTAs, indicating that our proposed network indeed enhances feature representations and obtains high-quality image information.

4.3. Feature Fusion Analysis

In this section, we discuss the performance of Adaptive Fusion Mechanism. We introduce four learnable weights, *i.e.*, λ_{conv}^{cls} , λ_{fc}^{cls} , λ_{conv}^{reg} , and λ_{fc}^{reg} in Eq. (2) and Eq. (4), to control the contributions of encoded *conv* and *fc* feature components from two paths to the fused output features in DQE and DAG shown in Fig.3. Obviously, larger λ_i^j with

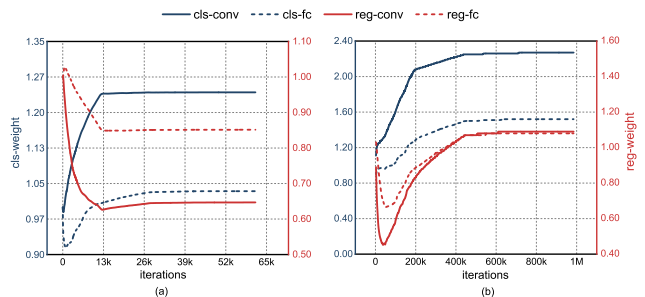


Figure 5. Performance visualization of our proposed Adaptive Fusion Mechanism. We plot values of four learnable weights, *i.e.*, λ_{conv}^{cls} , λ_{fc}^{cls} , λ_{conv}^{reg} , and λ_{fc}^{reg} against number of training iterations on: (a) PASCAL VOC in the first split, (b) MS COCO, in the base training phase. *cls-conv*, *cls-fc*, *reg-conv*, *reg-fc* indicate λ_{conv}^{cls} , λ_{fc}^{cls} , λ_{conv}^{reg} , and λ_{fc}^{reg} , respectively.

$i \in \{conv, fc\}$, $j \in \{cls, reg\}$ indicates that extractor *i* dominates the subtask *j* in feature extraction.

We visualize the variance of these four weights in base training phase ($K = 200$) on PASCAL VOC and MS COCO benchmarks, as shown in Fig. 5. As for PASCAL VOC, it is illustrated that the stabilizing value of λ_{conv}^{cls} is larger than λ_{fc}^{cls} while λ_{conv}^{reg} is lower compared with λ_{fc}^{reg} , representing that *conv* extractor dominates the classification subtask but is less important than *fc* extractor in bounding box regression in this experimental setup. Besides, we note that λ_i^{cls} with $i \in \{conv, fc\}$ in classification subtask is larger than λ_i^{reg} with $i \in \{conv, fc\}$ in regression sub-

Ablation	cls-conv	cls-fc	reg-conv	reg-fc	Novel AP_{50}
1		✓	✓		49.9
2	✓			✓	56.2
3	✓		✓		55.5
4		✓		✓	55.1
5	✓	✓		✓	59.1
6	✓	✓	✓		57.6
7	✓		✓	✓	59.0
8	✓	✓	✓	✓	60.7

Table 4. Ablation study on effectiveness of feature fusion. Comparison results among various fusion combinations in terms of AP_{50} for novel categories on Novel Set 1 of PASCAL VOC dataset are reported.

task respectively, indicating that performing classification generally needs more information than location estimation. When it comes to MS COCO, *conv* extractor consistently leads the classification subtask while these two kinds of extractors almost have equal contributions to bounding box regression. Besides, all these four weights when stabilizing are larger than those in the experiments on PASCAL VOC respectively, showing that training on complex MS COCO dataset generally requires richer information. Analysis above validates the efficacy of Adaptive Fusion Mechanism when facing distinct subtasks and datasets.

4.4. Ablation Study

In this section, we conduct relative ablations in 3/10-shot scenarios on the first base/novel split of PASCAL VOC. Results in all experiments are obtained by averaging over multiple random runs.

Effect of fusion. To examine the effectiveness of Adaptive Fusion Mechanism in Dual Query Encoder and Dual Attention Generator, we compare the performance of various feature fusion combinations and report AP_{50} of novel classes in 10-shot setup, as shown in Tabel 4, where $j-i, j \in \{cls, reg\}, i \in \{conv, fc\}$ in the header represents applying extractor i in subtask j . The existence of two extractors within a branch indicates that the information fusion is applied (*e.g.*, the regression branch in Fig.3 can be represented by “*reg-fc & reg-conv*”). In *Ablation 1-4*, we adopt only one extractor in each branch without feature fusion. Among these four experiments, “*cls-conv & reg-fc*” achieves the best performance, while “*cls-fc & reg-conv*” performs the worst, indicating that *conv* extractor prefers classification and *fc* extractor is more suitable for bounding box regression in the first split on PASCAL VOC dataset. This is consistent with the observations in Section 4.3. In *Ablation 5-7*, feature fusion is adopted in only one branch and boost the detection performance, suggesting that leveraging information from unfocused tasks is essential in each subtask. Applying feature fusion in both branches shown in

Shots	meta-cls	meta-reg	Base AP_{50}	Novel AP_{50}
3			68.3	43.1
	✓		67.8	44.2
	✓	✓	68.8	47.7
10			70.8	57.3
	✓		70.3	58.9
		✓	70.8	58.4
	✓	✓	70.6	60.7
	✓	✓	70.6	60.7

Table 5. Ablation study on effectiveness of meta losses. Comparison results among various meta loss combinations in terms of AP_{50} for both base and novel categories on Novel Set 1 of PASCAL VOC dataset are reported.

Ablation 8 obtains the best performance, further verifying the effectiveness of Adaptive Fusion Mechanism.

Effect of meta loss. In our approach, we further divide meta loss L_{meta} introduced in [44] into task-specific meta losses, *i.e.*, $L_{meta-cls}$ for classification and $L_{meta-reg}$ for bounding box regression. Similarly, we evaluate the effect of meta losses in Table 5. Obviously, both of the introduced $L_{meta-cls}$ and $L_{meta-reg}$ can indeed improve the performance on novel classes in K -shot setups. Besides, they provide similar contributions individually in robust 10-shot setup, while $L_{meta-reg}$ outperforms in relatively extreme (3-shot) scenario in comparison with $L_{meta-cls}$, probably suggesting that bounding box regression matters more when performing more strict few-shot object detection. Interestingly, the existence of meta losses almost have no positive influence on the detection of base classes. We believe the reason is that the few-shot detector has already been able to detect objects from base classes after base training phase with abundant annotations, despite the lack of meta losses.

5. Conclusion and Future Work

This work targets the problem of few-shot object detection. We carefully analyzed the characteristics of FSOD and presented that a general few-shot detector should: 1) explicitly decompose the processing of classification and localization; 2) fuse information from both subtasks for enhanced feature representations. Based on our observations, we proposed Adaptive Fully-Dual Network that performs two subtasks separately, involving feature representations, module reweighting, and decision making. For the acquisition of enhanced features, we proposed a novel Adaptive Fusion Mechanism. Despite its simplicity, our approach achieved significant performance on multiple benchmarks, demonstrating its effectiveness and generalization ability. It is worth noting that, our proposed framework and feature fusion mechanism are general, thus can be potentially applied into other two-stage or even one-stage models.

References

- [1] Marcin Andrychowicz, Misha Denil, Sergio Gomez, Matthew W Hoffman, David Pfau, Tom Schaul, Brendan Shillingford, and Nando De Freitas. Learning to learn by gradient descent by gradient descent. In *Advances in neural information processing systems*, pages 3981–3989, 2016. 1, 2
- [2] Luca Bertinetto, João F Henriques, Jack Valmadre, Philip Torr, and Andrea Vedaldi. Learning feed-forward one-shot learners. In *Advances in neural information processing systems*, pages 523–531, 2016. 2
- [3] Alexey Bochkovskiy, Chien-Yao Wang, and Hong-Yuan Mark Liao. Yolov4: Optimal speed and accuracy of object detection. *arXiv preprint arXiv:2004.10934*, 2020. 2
- [4] Zhaowei Cai and Nuno Vasconcelos. Cascade r-cnn: Delving into high quality object detection. In *Proceedings of the IEEE conference on computer vision and pattern recognition*, pages 6154–6162, 2018. 1
- [5] Hao Chen, Yali Wang, Guoyou Wang, and Yu Qiao. Lstd: A low-shot transfer detector for object detection. *arXiv preprint arXiv:1803.01529*, 2018. 2, 5, 6, 7
- [6] Wei-Yu Chen, Yen-Cheng Liu, Zsolt Kira, Yu-Chiang Frank Wang, and Jia-Bin Huang. A closer look at few-shot classification. *arXiv preprint arXiv:1904.04232*, 2019. 2
- [7] Yinbo Chen, Xiaolong Wang, Zhuang Liu, Huijuan Xu, and Trevor Darrell. A new meta-baseline for few-shot learning. *arXiv preprint arXiv:2003.04390*, 2020. 2
- [8] Jifeng Dai, Yi Li, Kaiming He, and Jian Sun. R-fcn: Object detection via region-based fully convolutional networks. In *Advances in neural information processing systems*, pages 379–387, 2016. 1, 2
- [9] Jifeng Dai, Haozhi Qi, Yuwen Xiong, Yi Li, Guodong Zhang, Han Hu, and Yichen Wei. Deformable convolutional networks. In *Proceedings of the IEEE international conference on computer vision*, pages 764–773, 2017. 1
- [10] Qi Fan, Wei Zhuo, Chi-Keung Tang, and Yu-Wing Tai. Few-shot object detection with attention-rpn and multi-relation detector. In *Proceedings of the IEEE/CVF Conference on Computer Vision and Pattern Recognition*, pages 4013–4022, 2020. 2, 5, 7
- [11] Chelsea Finn, Pieter Abbeel, and Sergey Levine. Model-agnostic meta-learning for fast adaptation of deep networks. In *ICML*, 2017. 1, 2
- [12] Spyros Gidaris and Nikos Komodakis. Dynamic few-shot visual learning without forgetting. In *Proceedings of the IEEE Conference on Computer Vision and Pattern Recognition*, pages 4367–4375, 2018. 1, 2
- [13] Ross Girshick. Fast r-cnn. In *Proceedings of the IEEE international conference on computer vision*, pages 1440–1448, 2015. 1, 2
- [14] Ross Girshick, Jeff Donahue, Trevor Darrell, and Jitendra Malik. Rich feature hierarchies for accurate object detection and semantic segmentation. In *Proceedings of the IEEE conference on computer vision and pattern recognition*, pages 580–587, 2014. 1, 2
- [15] Kaiming He, Georgia Gkioxari, Piotr Dollár, and Ross Girshick. Mask r-cnn. In *Proceedings of the IEEE international conference on computer vision*, pages 2961–2969, 2017. 6
- [16] Kaiming He, Xiangyu Zhang, Shaoqing Ren, and Jian Sun. Spatial pyramid pooling in deep convolutional networks for visual recognition. *IEEE transactions on pattern analysis and machine intelligence*, 37(9):1904–1916, 2015. 2
- [17] Kaiming He, Xiangyu Zhang, Shaoqing Ren, and Jian Sun. Deep residual learning for image recognition. In *Proceedings of the IEEE conference on computer vision and pattern recognition*, pages 770–778, 2016. 1, 6
- [18] Gao Huang, Zhuang Liu, Laurens Van Der Maaten, and Kilian Q Weinberger. Densely connected convolutional networks. In *Proceedings of the IEEE conference on computer vision and pattern recognition*, pages 4700–4708, 2017. 1
- [19] Bingyi Kang, Zhuang Liu, Xin Wang, Fisher Yu, Jiashi Feng, and Trevor Darrell. Few-shot object detection via feature reweighting. In *Proceedings of the IEEE International Conference on Computer Vision*, pages 8420–8429, 2019. 1, 2, 3, 4, 5, 6, 7
- [20] Leonid Karlinsky, Joseph Shtok, Sivan Harary, Eli Schwartz, Amit Aides, Rogerio Feris, Raja Giryes, and Alex M Bronstein. Repmet: Representative-based metric learning for classification and few-shot object detection. In *Proceedings of the IEEE Conference on Computer Vision and Pattern Recognition*, pages 5197–5206, 2019. 2
- [21] Gregory Koch, Richard Zemel, and Ruslan Salakhutdinov. Siamese neural networks for one-shot image recognition. In *ICML deep learning workshop*, volume 2. Lille, 2015. 1, 2
- [22] Brenden M Lake, Ruslan Salakhutdinov, and Joshua B Tenenbaum. Human-level concept learning through probabilistic program induction. *Science*, 350(6266):1332–1338, 2015. 1, 2
- [23] Tsung-Yi Lin, Piotr Dollár, Ross Girshick, Kaiming He, Bharath Hariharan, and Serge Belongie. Feature pyramid networks for object detection. In *Proceedings of the IEEE conference on computer vision and pattern recognition*, pages 2117–2125, 2017. 1, 2
- [24] Wei Liu, Dragomir Anguelov, Dumitru Erhan, Christian Szegedy, Scott Reed, Cheng-Yang Fu, and Alexander C Berg. Ssd: Single shot multibox detector. In *European conference on computer vision*, pages 21–37. Springer, 2016. 2, 5
- [25] Alex Nichol, Joshua Achiam, and John Schulman. On first-order meta-learning algorithms. *arXiv preprint arXiv:1803.02999*, 2018. 1, 2
- [26] Adam Paszke, Sam Gross, Soumith Chintala, Gregory Chanan, Edward Yang, Zachary DeVito, Zeming Lin, Alban Desmaison, Luca Antiga, and Adam Lerer. Automatic differentiation in pytorch. 2017. 6
- [27] Siyuan Qiao, Chenxi Liu, Wei Shen, and Alan L Yuille. Few-shot image recognition by predicting parameters from activations. In *Proceedings of the IEEE Conference on Computer Vision and Pattern Recognition*, pages 7229–7238, 2018. 1
- [28] Sachin Ravi and Hugo Larochelle. Optimization as a model for few-shot learning. 2016. 2

- [29] Joseph Redmon, Santosh Divvala, Ross Girshick, and Ali Farhadi. You only look once: Unified, real-time object detection. In *Proceedings of the IEEE conference on computer vision and pattern recognition*, pages 779–788, 2016. 1, 2
- [30] Joseph Redmon and Ali Farhadi. Yolo9000: better, faster, stronger. In *Proceedings of the IEEE conference on computer vision and pattern recognition*, pages 7263–7271, 2017. 1, 2
- [31] Joseph Redmon and Ali Farhadi. Yolov3: An incremental improvement. *arXiv preprint arXiv:1804.02767*, 2018. 2, 5
- [32] Shaoqing Ren, Kaiming He, Ross Girshick, and Jian Sun. Faster r-cnn: Towards real-time object detection with region proposal networks. In *Advances in neural information processing systems*, pages 91–99, 2015. 1, 2, 3
- [33] Olga Russakovsky, Jia Deng, Hao Su, Jonathan Krause, Sanjeev Satheesh, Sean Ma, Zhiheng Huang, Andrej Karpathy, Aditya Khosla, Michael Bernstein, et al. Imagenet large scale visual recognition challenge. *International journal of computer vision*, 115(3):211–252, 2015. 6
- [34] Larissa K Samuelson and Linda B Smith. They call it like they see it: Spontaneous naming and attention to shape. *Developmental Science*, 8(2):182–198, 2005. 1
- [35] Jake Snell, Kevin Swersky, and Richard Zemel. Prototypical networks for few-shot learning. In *Advances in neural information processing systems*, pages 4077–4087, 2017. 1, 2
- [36] Flood Sung, Yongxin Yang, Li Zhang, Tao Xiang, Philip HS Torr, and Timothy M Hospedales. Learning to compare: Relation network for few-shot learning. In *Proceedings of the IEEE Conference on Computer Vision and Pattern Recognition*, pages 1199–1208, 2018. 1, 2
- [37] Oriol Vinyals, Charles Blundell, Timothy Lillicrap, Daan Wierstra, et al. Matching networks for one shot learning. In *Advances in neural information processing systems*, pages 3630–3638, 2016. 1, 2
- [38] Xin Wang, Thomas E Huang, Trevor Darrell, Joseph E Gonzalez, and Fisher Yu. Frustratingly simple few-shot object detection. *arXiv preprint arXiv:2003.06957*, 2020. 2, 5, 6, 7
- [39] Xin Wang, Fisher Yu, Ruth Wang, Trevor Darrell, and Joseph E Gonzalez. Tafe-net: Task-aware feature embeddings for low shot learning. In *Proceedings of the IEEE Conference on Computer Vision and Pattern Recognition*, pages 1831–1840, 2019. 2
- [40] Yu-Xiong Wang, Deva Ramanan, and Martial Hebert. Meta-learning to detect rare objects. In *Proceedings of the IEEE International Conference on Computer Vision*, pages 9925–9934, 2019. 3, 5, 6, 7
- [41] Yue Wu, Yinpeng Chen, Lu Yuan, Zicheng Liu, Lijuan Wang, Hongzhi Li, and Yun Fu. Rethinking classification and localization for object detection. In *Proceedings of the IEEE/CVF Conference on Computer Vision and Pattern Recognition*, pages 10186–10195, 2020. 2
- [42] Yang Xiao and Renaud Marlet. Few-shot object detection and viewpoint estimation for objects in the wild. In *European Conference on Computer Vision (ECCV)*, 2020. 1, 3, 4, 5, 6, 7
- [43] Yinda Xu, Zeyu Wang, Zuoxin Li, Ye Yuan, and Gang Yu. Siamfc++: Towards robust and accurate visual tracking with target estimation guidelines. In *AAAI*, pages 12549–12556, 2020. 2
- [44] Xiaopeng Yan, Ziliang Chen, Anni Xu, Xiaoxi Wang, Xiaodan Liang, and Liang Lin. Meta r-cnn: Towards general solver for instance-level low-shot learning. In *Proceedings of the IEEE International Conference on Computer Vision*, pages 9577–9586, 2019. 1, 3, 4, 5, 6, 7, 8
- [45] Chiyuan Zhang, Samy Bengio, Moritz Hardt, Benjamin Recht, and Oriol Vinyals. Understanding deep learning requires rethinking generalization. *arXiv preprint arXiv:1611.03530*, 2016. 1